Environmental Science & Technology

Article

pubs.acs.org/est

Fe(II) Uptake on Natural Montmorillonites. I. Macroscopic and Spectroscopic Characterization

Daniela Soltermann,*[,†,‡] Maria Marques Fernandes,[†] Bart Baeyens,[†] Rainer Dähn,[†] Prachi A. Joshi,[§] Andreas C. Scheinost,[∥,○] and Christopher A. Gorski[§]

[†]Laboratory for Waste Management, Paul Scherrer Institut, 5232 Villigen PSI, Switzerland

[‡]Institute of Biogeochemistry and Pollutant Dynamics, ETH Zürich, 8092 Zürich, Switzerland

[§]Department of Civil and Environmental Engineering, Pennsylvania State University, University Park, Pennsylvania 16802, United States

[∥]Institute of Resource Ecology, Helmholtz-Zentrum Dresden-Rossendorf e.V., 01328 Dresden, Germany

[○]The Rossendorf Beamline at ESRF, P.O. Box 220, F-38043 Grenoble, France

Supporting Information

ABSTRACT: Iron is an important redox-active element that is ubiquitous in both engineered and natural environments. In this study, the retention mechanism of Fe(II) on clay minerals was investigated using macroscopic sorption experiments combined with Mössbauer and extended X-ray absorption fine structure (EXAFS) spectroscopy. Sorption edges and isotherms were measured under anoxic conditions on natural Fe-bearing montmorillonites (STx, SWy, and SWa) having different structural Fe contents ranging from 0.5 to 15.4 wt % and different initial Fe redox states. Batch experiments indicated that, in the case of low Fe-bearing (STx) and dithionite-reduced clays, the Fe(II) uptake follows the sorption behavior of other divalent transition metals, whereas Fe(II) sorption increased by up to 2 orders of magnitude on the unreduced, Fe(III)-rich montmorillonites (SWy and SWa). Mössbauer spectroscopy analysis revealed that nearly all the sorbed Fe(II) was oxidized to surface-bound Fe(III) and secondary Fe(III) precipitates were formed on the Fe(III)-rich montmorillonite, while sorbed Fe is predominantly present as Fe(II) on Fe-low and dithionite-reduced clays. The results provide compelling evidence that Fe(II) uptake characteristics on clay minerals are strongly correlated to the redox properties of the structural Fe(III). The improved understanding of the interfacial redox interactions between sorbed Fe(II) and clay minerals gained in this study is essential for future studies developing Fe(II) sorption models on natural montmorillonites.

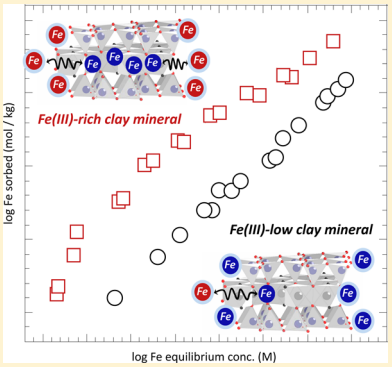

INTRODUCTION

Iron species associated with clay minerals are of great relevance for the biogeochemical cycling of metals and the fate of contaminants.[1−3] Structural iron in the clay lattice is a strong redox buffer which can act as both electron acceptor and donor, representing an important natural reductant for inorganic and organic pollutants and oxidant for metal- and sulfate-reducing bacteria.[1,4−8] For Fe-bearing clay minerals, it has been demonstrated that redox-active Fe(II) is predominantly present as structural Fe(II) or Fe(II) bound to the clay platelet edge sites.[1] Despite the large body of existing work investigating the reactivity of structural Fe in clay mineral lattices,[3−5,9,10] a molecular-level understanding and description of the interfacial interactions of dissolved Fe(II) with clay mineral surfaces is still lacking. Assessing the Fe(II) uptake processes on 2:1 dioctahedral clay minerals has proven to be challenging due to the experimental difficulty in carrying out measurements under well-defined anoxic conditions. Moreover, spectra of sorbed Fe(II) in advanced spectroscopic techniques, such as extended X-ray absorption fine structure (EXAFS) spectroscopy, are significantly impaired by the presence of the iron in the clay structure.

Previous studies have mainly addressed the reactivity of Fe(II) sorbed or precipitated on Fe(III)-containing minerals such as green rust, goethite, lepidocrocite, or ferric iron hydroxide,[11−14] while the effect and sorption behavior of Fe(II) taken up by natural clay minerals has received less attention.[5,15,16] Fe(II) uptake measurements on Fe-bearing clay minerals (e.g., NAu and SWa)[15,17] indicated that the concentration and pH dependent sorption of Fe(II) is clearly stronger than expected for divalent transition metals such as Ni and Zn.[18] While an explanation for the increased sorption values on natural clays is still missing, it seems plausible that this effect may be assigned to an electron transfer between sorbed Fe(II) and structural Fe(III), as previously shown for NAu nontronite at high iron loadings (~710 mmol kg^{-1}).[2,19]

Received: April 16, 2014
Revised: June 13, 2014
Accepted: June 15, 2014
Published: June 16, 2014

   dx.doi.org/10.1021/es501887q | Environ. Sci. Technol. 2014, 48, 8688−8697

To date, evidence for this mechanism is scattered among different Fe-bearing minerals, such as hematite, goethite, and magnetite under only a narrow range of conditions.[20−22] To develop a stronger understanding of the relationship between the Fe(II) sorption and Fe(II)/Fe(III) redox reactions, particularly at low Fe(II) surface loadings, systematic investigations under a well-defined range of conditions and on clay minerals having different structural Fe properties are necessary.

The aim of this work is to obtain an enhanced understanding of the influence of the structural Fe and its redox state on Fe(II) sorption processes and to relate the extent of Fe(II) uptake to newly formed Fe surface species. To this end, the best approach to assess the Fe(II) uptake behavior at the clay−water interface is to combine macroscopic sorption experiments and spectroscopic techniques. Here, the sorption of Fe(II) was investigated by combining batch sorption experiments with Mössbauer and EXAFS spectroscopic measurements. From the mechanistic understanding of the Fe(II) uptake gained in this study, an improved sorption model of Fe(II) on natural 2:1 dioctahedral clay minerals has been developed in a companion paper.[23] Results from batch sorption experiments combined with surface analytical techniques will be used to improve sorption models for describing the fate of Fe(II) in natural and engineered environments.

MATERIAL AND METHODS

Texas montmorillonite (STx-1), Wyoming montmorillonite (SWy-2), and a ferruginous smectite (SWa-1) were obtained from the Source Clay Repository of the Clay Minerals Society (Purdue University, West Lafayette, IN) and are characterized by different structural Fe(III) contents of 0.5, 2.9, and 15.4 wt %, respectively. To prevent any redox interaction of structural Fe(III) with sorbed Fe(II), a synthetic Fe-free montmorillonite (IFM) and a dithionite-reduced SWy (red SWy) were used. Details on the synthesis and treatment of IFM were provided in previous studies.[24−26] The purification and size fractionation of the montmorillonites, as well as the anoxic conditions used in the experiments have been described previously.[27,28] The cation exchange capacity of the natural, synthetic, and dithionite-reduced clays were determined by the ^{134}Cs isotopic dilution method[29] (Table S1 in the Supporting Information). Batch sorption experiments were carried out on all the clay minerals mentioned, whereas only two of them, STx and SWy montmorillonite, were investigated by Mössbauer and EXAFS spectroscopy in this study.

Dithionite-Reduced Montmorillonite. A completely dithionite-reduced SWy (red SWy) was prepared following the standard procedure of Stucki et al.[30] A 75 mL portion of the clay suspension (sorbent concentration 5 g L^{-1}) was diluted in a citrate-bicarbonate buffer solution (1.6 mL 0.5 M $Na_3C_6H_5O_7{\cdot}2H_2O$ and 23.4 mL of 1 M $NaHCO_3$). After heating the clay suspension to ∼70 °C, sodium dithionite ($Na_2S_2O_4$), corresponding to three times the mass of clay, was added to the stock solution and reacted overnight. The dithionite-treated clay suspension was subsequently loaded into Visking dialysis bags and shaken end-over-end together with deoxygenated 0.1 M $NaClO_4$. The $NaClO_4$ solution was exchanged eight times until the reductants, related ions, and salts were removed from the clay suspensions. The change in oxidation state of the structural Fe following dithionite treatment was determined using Mössbauer spectroscopy.

Fe(II) Batch Sorption Experiments. All sorption experiments were carried out in a glovebox under controlled N_2 atmosphere (O_2 < 0.1 ppm) at 25 ± 1 °C. To avoid any oxygen contamination, sampling materials and polycarbonate centrifuge tubes were evacuated overnight in the vacuum chamber and allowed to equilibrate in the N_2 atmosphere prior to use. Clay suspensions and aqueous solutions were deoxygenated by heating to 60−100 °C and purging with Ar gas for at least 3 h prior to transferring them into the glovebox. Source radiotracer solutions of ^{55}Fe(III) were purchased from Eckert & Ziegler Isotope Products, Valencia, CA. The labeled ^{55}Fe(III) solutions were reduced to ^{55}Fe(II) in an electrochemical cell (E_h = −0.44 V vs SHE) containing a cylindrical glassy carbon working electrode (Sigradur G, HTW, Germany), a platinum wire counter electrode and an Ag/AgCl reference electrode (Bioanalytical In., West Lafayette, IN).

Sorption edge measurements as a function of pH at trace radionuclide concentrations (<10^{-7} M) were performed in 0.1 M $NaClO_4$ background electrolyte (sorbent concentration ∼1 g L^{-1}). In order to maintain constant pH conditions, the experiments were buffered with sodium acetate (pH 3.5−4.5), MES (2-(*N*-morpholino)ethanesulfonic acid, pH 5.5−6.5), MOPS (3-(*N*-morpholino)propanesulfonic acid, pH 7.0−7.5), TRIS (tris (hydroxymethyl)aminomethane, pH 8.0−8.5), or CHES (*N*-cyclohexyl-2-aminoethanesulfonic acid, pH 9.0−9.5) at concentrations of 2 × 10^{-3} M. In previous experiments, no metal ion complexation with the above-mentioned buffers was observed (e.g., Ni and Zn).[31,32] Specific experiments to check their influence on the interaction of Fe(II) with clay mineral surfaces were not carried out in this study. However, the agreement between sorption measurements of Zn(II) and Fe(II) on synthetic IFM[26] argues against potential effects of the buffers on the Fe(II) uptake. Clay suspensions were prepared in 25 mL polycarbonate centrifuge tubes and labeled with the electrochemically reduced ^{55}Fe(II) tracer. The samples were shaken end-over-end for at least 3 days followed by phase separation by centrifugation using a Beckman-Coulter Ultracentrifuge (Beckman Coulter, Krefeld, Germany) inside the glovebox at 105 000g_{max}. The solid liquid distribution ratio R_d was determined by measuring the ^{55}Fe activity in the supernatant solution using a Tri-Carb 2750 TR/LL liquid scintillation analyzer (Canberra Packard, Schwadorf, Austria) and is defined as follows:

$$R_d = \frac{c_{in} - c_{eq}}{c_{eq}} \frac{V}{m} \ (\mathrm{L\ kg^{-1}}) \tag{1}$$

where c_{in} is the total initial aqueous Fe(II) concentration, c_{eq} is the total equilibrium Fe(II) concentration, V is the volume of liquid phase, and m is the mass of the solid phase. To better reflect the sensitivity of the sorption to changing conditions and to illustrate the sorption independency of the solid-to-liquid distribution ratio chosen, the sorption edge data were plotted as the logarithm of the distribution ratio R_d against pH.[33] The same experimental procedure was used for the concentration dependent measurements (sorption isotherm) except that the pH value was adjusted to 6.2 and the initial Fe(II) concentration varied between 10^{-7} and 10^{-3} M. For this type of experiments the quantity of sorbed Fe (mol kg^{-1}) was plotted against the Fe equilibrium concentrations (M).

Mössbauer and EXAFS Analyses. For the Mössbauer and EXAFS investigations additional Fe(II) sorption experiments were conducted at sorbent concentrations of 7.5 g L^{-1} in 0.1 M

dx.doi.org/10.1021/es501887q | Environ. Sci. Technol. 2014, 48, 8688−8697

Table 1. Fe Analysis of Texas (STx) and Wyoming (SWy) Montmorillonite Samples Investigated by ^{57}Fe Mössbauer and EXAFS Spectroscopy

		structural Fe		sorbed Fe	structural Fe	
		wt %	mmol kg^{-1}	mmol kg^{-1}	% of total Fe[c]	
					Mössbauer ^{57}Fe	EXAFS Fe
			red SWy			
^{57}Fe red SWy	^{57}Fe(II) reacted[a]	2.8(0.1)	496.6	40.7	18.4	
^{56}Fe red SWy	^{56}Fe(II) reacted[a]	2.8(0.1)	496.6	64.6	98.4	
			STx			
^{57}Fe STx a	^{57}Fe(II) reacted[a]	0.5(0.1)	96.4	9.5	15.7	
^{57}Fe STx b	^{57}Fe(II) reacted[a]	0.5(0.1)	96.4	39.8	4.2	
^{56}Fe STx b	^{56}Fe(II) reacted[a]	0.5(0.1)	96.4	44.7	99.9	
Fe STx c	Fe(II) reacted[b]	0.5(0.1)	96.4	114.8		45.6
			SWy			
^{57}Fe SWy a	^{57}Fe(II) reacted[a]	2.9(0.1)	520.6	49.0	16.4	
^{57}Fe SWy b	^{57}Fe(II) reacted[a]	2.9(0.1)	520.6	128.8	6.9	
^{56}Fe SWy b	^{56}Fe(II) reacted[a]	2.9(0.1)	520.6	125.9	99.9	
Fe SWy c	Fe(II) reacted[b]	2.9(0.1)	520.6	195.0		72.6

[a]^{57}Fe Mössbauer spectroscopy. [b]EXAFS spectroscopy. [c]Fraction of the total spectroscopic signal resulting from the structural ^{57}Fe or total Fe for Mössbauer and EXAFS measurements, respectively.

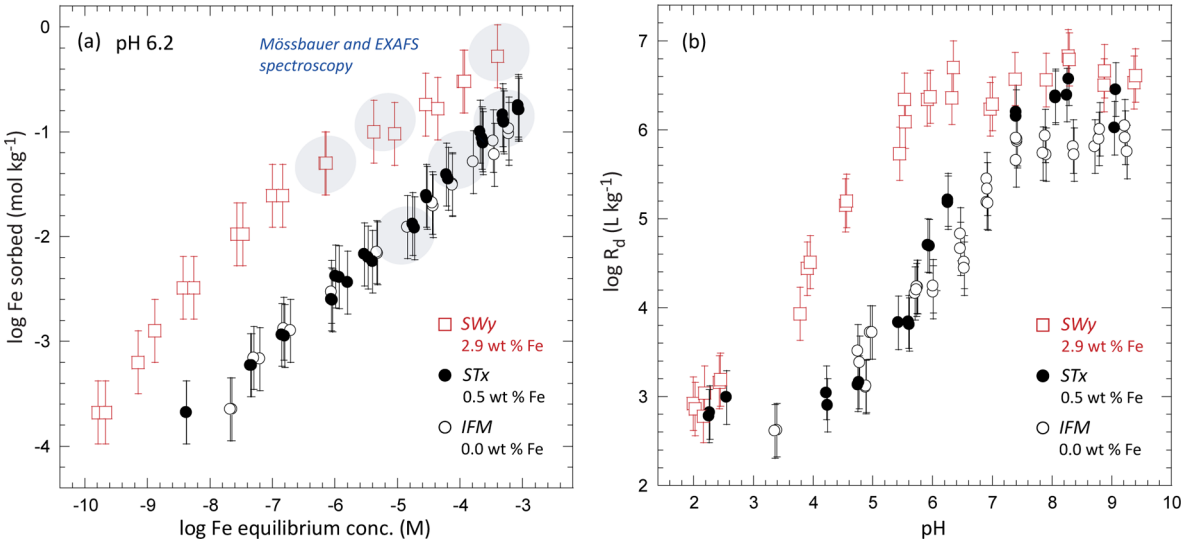

Figure 1. (a) Sorption isotherm data of Fe(II) on natural SWy (open squares), STx (closed circles), and synthetic IFM (open circles) at pH 6.2 in 0.1 M $NaClO_4$ (sorbent concentration of 1 g L^{-1}). (b) Fe(II) sorption edge data on SWy, STx, and IFM in 0.1 M $NaClO_4$ ($Fe_{tot} = 3 \times 10^{-8}$ M). R_d denotes the solid liquid distribution ratio as defined in eq 1. EXAFS and Mössbauer samples and their corresponding Fe loadings are encircled.

$NaClO_4$ at pH 6.2 (Table 1). After equilibration, the clay suspensions were centrifuged, the supernatant was discarded and the remaining wet clay paste was sealed between two pieces of Kapton tape, taken out from the glovebox, and immediately shock frozen with liquid N_2. Mössbauer measurements were collected at 12 K and the data were analyzed with Recoil software (Ottawa, Canada) using Voigt-based fitting.[34] ^{57}Fe(II) enriched stock solutions (97.83% ^{57}Fe) were used to enhance the isotopic-specific ^{57}Fe Mössbauer signal. To investigate changes in the structural ^{57}Fe of naturally occurring clay minerals, identical samples were prepared using enriched ^{56}Fe(II) stock solutions (99.77% ^{56}Fe). The fraction of the total signal resulting from the structural ^{57}Fe is summarized in Table 1.

EXAFS samples were prepared under identical conditions as for the Mössbauer measurements (Table 1, *Fe STx c* and *Fe SWy c*). However, in contrast to the Mössbauer technique, EXAFS is not ^{57}Fe isotope specific which means that the spectra obtained will be a mixture of both structural and sorbed Fe species. For this reason, the EXAFS spectra of the structural Fe was recorded as a reference to analyze the Fe surface complexes. The Fe K-edge EXAFS spectra were collected at the Rossendorf Beamline (ROBL) at the European Synchrotron Radiation Facility (ESRF) in Grenoble (France), using a Si(111) double crystal for monochromatization and Si mirror for suppression of higher harmonics. Fluorescence spectra were measured using a 13 element high-purity Ge-detector (Canberra) with digital signal analyzer (XIA-XMAP). O_2 diffusion into the polyethylene sample holders was minimized by transporting them in a Dewar filled with liquid N_2 to the synchrotron facility. The frozen samples were measured in a closed-cycle He-cryostat at 15 K to exclude oxygen and to improve signal quality by eliminating thermal contributions to the Debye–Waller factor. EXAFS data reduction and fitting

dx.doi.org/10.1021/es501887q | Environ. Sci. Technol. 2014, 48, 8688–8697

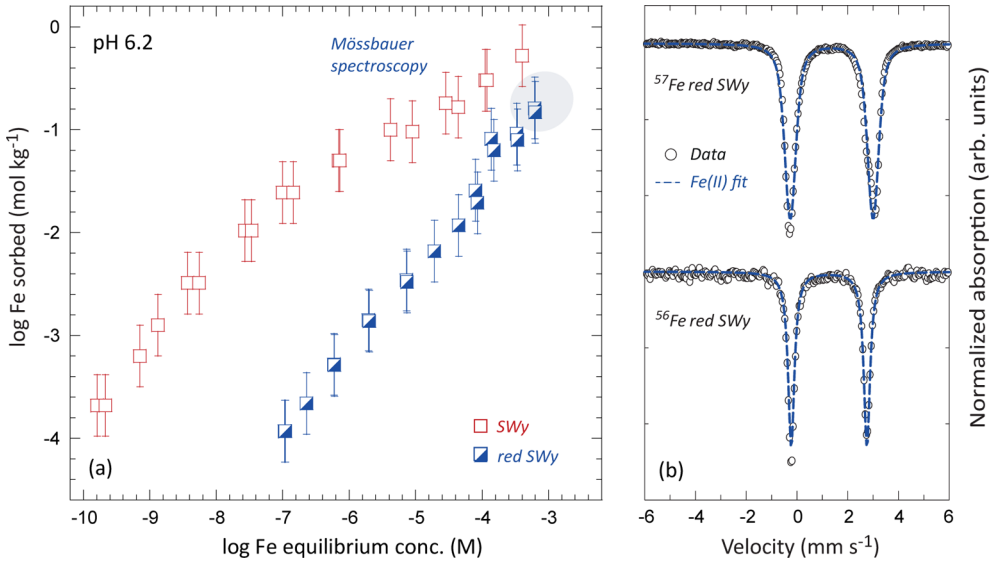

Figure 2. (a) Fe(II) sorption isotherm on natural SWy (open squares) and dithionite-reduced SWy (red SWy, ~100% structural Fe(II), semisquares) at pH 6.2 in 0.1 M $NaClO_4$ (sorbent concentration of 1 g L^{-1}). (b) Mössbauer spectra of red SWy reacted with ^{57}Fe(II) (40.7 mmol kg^{-1} sorbed ^{57}Fe, spectra above) and invisible ^{56}Fe(II) (64.6 mmol kg^{-1} sorbed ^{56}Fe, spectra below). ^{56}Fe is transparent to ^{57}Fe Mössbauer spectroscopy and was used to monitor changes in the oxidation state of ^{57}Fe present in the clay structure.

were performed with the Athena/Artemis interface of IFEFFIT software[35,36] following standard procedures. Details about the EXAFS fit approach are given in Section S2 and S3 of the Supporting Information (SI).

RESULTS AND DISCUSSION

Two lines of experiments were used to investigate whether Fe(II) uptake behavior depends (i) on the structural Fe(III) content of the different clays and/or (ii) on the initial redox state of the structural Fe. The former was studied by carrying out sorption experiments on natural montmorillonites exhibiting different structural Fe(III) contents. The latter was investigated using oxidized and dithionite-reduced clays.

Fe(II) Uptake on Natural Montmorillonites. To investigate whether the Fe(II) uptake behavior depends on the Fe content of the clay, Fe(II) sorption isotherm and edge measurements were performed on montmorillonites with structural Fe(III) contents of 0.0 wt % (IFM), 0.5 wt % (STx), 2.9 wt % (SWy), and 15.4 wt % (SWa). The concentration dependent uptake of Fe(II) on the low Fe-content STx is in excellent agreement with the measurements on the synthetic Fe-free IFM (black vs open circles in Figure 1a). The pH-dependent sorption of Fe(II) is within the errors of log R_d ± 0.3 L kg^{-1} similar on STx and IFM (sorption edge in Figure 1b). The strong pH dependency of the R_d values between pH 4.5 and 7.5 is typical for surface complexation of metal cations at the "broken bond" surfaces or clay mineral edge sites.[18,27] As recently shown on IFM,[26] the uptake of Fe(II) follows well the sorption behavior of other divalent metals.

The interaction of Fe(II) with SWy (2.9 wt % Fe) yielded considerably higher sorption values than expected for divalent metals. In the isotherm at pH 6.2, the Fe(II) sorption is up to 1 order of magnitude stronger than for STx and IFM (open squares in Figure 1a). These results were unexpected since previous work found that the Zn(II) sorption isotherms on both STx and SWy were the same.[37,38] In addition, the pH-dependence of Fe(II) sorption on SWy is more pronounced (Figure 1b). The rise of the sorption edge begins at lower pH values and levels off at pH 6 (log R_d ~ 6.6 ± 0.3 L kg^{-1}). The results indicate that the uptake of Fe(II) on SWy is distinctly different from that of STx and synthetic clay. A plausible explanation for the enhanced sorption on SWy can be derived from recent work on nontronite[19] indicating that electron transfer reactions between sorbed Fe(II) and structural Fe(III) in the clay lattice might occur. To further test the influence of the structural Fe content on the Fe(II) sorption, an isotherm of Fe(II) was measured on a natural ferruginous smecite (SWa) having an iron content of 15.4 wt % (Figure S1 in the SI). The sorption results at pH 6.2 are within the expected error of ±0.3 log units consistent with the data on SWy (2.9 wt % Fe). This finding indicates that a significant stronger Fe(II) uptake may be expected on Fe-rich montmorillonites, although it is apparently not linearly correlated with the Fe(III) content.

Fe(II) Uptake on Dithionite-Reduced Montmorillonites. The obtained sorption data clearly show that there are significant differences in the Fe(II) uptake behavior between the natural Fe-low (STx) and Fe-rich (SWy and SWa) montmorillonites. In the latter, the Fe(II) sorption is much more pronounced.[2,19] If these high sorption values are induced by an interfacial electron transfer between sorbed Fe(II) and structural Fe(III) in the clay, we would expect that the Fe(II) uptake on dithionite-reduced montmorillonites (e.g., red SWy), where the structural Fe(III) is reduced to Fe(II), should be significantly lower. As shown in Figure 2a, the quantities of sorbed Fe(II) decrease by up to 2.2 ± 0.3 log units on the reduced SWy (the Fe(II) isotherm at pH 7.2 is shown in Figure S2 in the SI). A similar Fe(II) uptake behavior has been observed for the dithionite-reduced SWa (~84.2 ± 2.4% structural Fe(II), Figure S3 in the SI).

Mössbauer Analysis of Dithionite-Reduced SWy. Wet chemistry data alone cannot resolve why unexpected high sorption values are observed for certain clay minerals (SWy and SWa) and not for others (STx, IFM and red SWy). The oxidation state of the sorbed Fe(II) on red SWy samples was therefore verified by Mössbauer spectroscopy (shaded area in

dx.doi.org/10.1021/es501887q | Environ. Sci. Technol. 2014, 48, 8688−8697

Table 2. Mössbauer Parameters for Untreated Montmorillonite References and Montmorillonites Reacted with ^{57}Fe(II) and ^{56}Fe(II), Respectively

	sorbed Fe mmol kg^{-1}	mineral	IS^a mm s^{-1}	QS^b mm s^{-1}	area %	contriubution %
			red SWy			
reference		Fe^{2+}	1.26	2.98		100
^{57}Fe red SWy	40.7	Fe^{2+}	1.37	3.27		100
^{56}Fe red SWy	64.6	Fe^{2+}	1.26	2.98		100
			STx			
reference		Fe^{3+}	0.45	0.93		100
^{57}Fe STx a	9.5	Fe^{2+}	1.38	3.22	40.2(2.3)	40.2
		Fe^{3+}	0.48	0.86	59.8(2.3)	59.8
^{57}Fe STx b	39.8	Fe^{2+}	1.38	3.44	68.8(3.3)	68.8
		Fe^{3+}	0.51	0.74	12.2(3.6)	31.1
		magnetite	0.47	−0.01	18.9(3.6)	
^{56}Fe STx b	44.7	Fe^{2+}	1.51	2.70	26.8(5.9)	26.8
		Fe^{3+}	0.34	0.98	73.2(5.9)	73.2
			SWy			
reference		Fe^{3+}	0.45	0.93		100
^{57}Fe SWy a	49.0	Fe^{2+}	1.23	3.06	2.0(4.2)	2.0
		Fe^{3+}	0.47	0.74	17.7(1.5)	98.0
		magnetite	0.52	−0.09	24.2(3.3)	
		magnetite	0.43	0.02	56.1(3.1)	
^{57}Fe SWy b	128.8	Fe^{2+}	1.36	3.21	9.3(2.2)	9.3
		Fe^{3+}	0.53	0.78	10.7(2.0)	90.6
		lepidocrocite	0.48	−0.03	79.9(2.7)	
^{56}Fe SWy b	125.9	Fe^{2+}	1.26	3.02	25.5(2.4)	25.5
		Fe^{3+}	0.40	2.31	74.5(2.4)	74.5

^{a}Center shift relative to α-Fe(0). ^{b}Quadrupole splitting.

Figure 2a). The spectra collected on red SWy with a ^{57}Fe(II) loading of ∼41 mmol kg^{-1} is shown at the top of Figure 2b. After Fe(II) sorption, the Mössbauer spectrum reveals a doublet peak (CS 1.37 mm s^{-1} and QS 3.27 mm s^{-1}) characteristic of mineral-bound Fe(II)[39] (Table 2). To check whether the structural Fe(II) remains unaffected, sorption experiments were carried out with Mössbauer invisible ^{56}Fe(II) (Figure 2b, below). The hyperfine parameters obtained coincide with the values for the reference without any sorbed Fe(II) which suggests that structural Fe(II) remains completely reduced (^{56}Fe red SWy vs reference in Table 2). The fact that an electron transfer to the structural Fe is unfeasible in case of IFM and red SWy makes it plausible that an interfacial electron transfer is hardly taking place on STx montmorillonite. To corroborate this hypothesis, isotope selective Mössbauer spectroscopy was performed on medium and high Fe loaded STx and SWy samples (shaded areas in Figure 1a).

Mössbauer Analysis of STx. STx samples were equilibrated with isotopically enriched ^{57}Fe(II) at pH 6.2 in order to monitor the Fe surface species. Mössbauer spectra were collected on samples with Fe loadings of 10 mmol kg^{-1} (^{57}Fe STx a) and 40 mmol kg^{-1} (^{57}Fe STx b). The spectra of ^{57}Fe STx a in Figure 3a shows two paramagnetic doublets: (i) one consistent with sorbed and/or structural ^{57}Fe(II) species (dashed lines) and (ii) the other consistent with Fe(III) (filled area) based on their hyperfine parameters. The Fe(II) doublets have slightly larger center shift (CS) and broader quadrupole splitting (QS) than typical structural and sorbed Fe(II) phases. However, the appearance of similar Fe(II) doublets has been observed for the ^{57}Fe(II) uptake on natural nontronite and synthetic montmorillonite[2,26] which has been attributed to an increase of Fe(II) outer-sphere complexes.[40,41] The results of the Mössbauer fits (Table 2) clearly demonstrate that sorbed Fe(II) is partly oxidized to Fe(III) on the clay surface (up to 60 ± 2%). Although STx was reacted with isotopically enriched ^{57}Fe(II), about 16% of the total spectral area still results from the intrinsic ^{57}Fe in the clay lattice (Table 1). Assuming that the structural ^{57}Fe is predominantly present as Fe(III), the fraction of surface-bound Fe(III) is therefore probably less than 60% of the total sorbed Fe (<6 mmol kg^{-1}).

The Mössbauer spectra of the ^{57}Fe STx b sample (Figure 3b) resembles the spectra of the ^{57}Fe STx a sample (Figure 3a). The hyperfine parameters of the lower loaded sample are within the errors comparable to the higher loaded sample, except that for the latter the ratio of surface-bound Fe(III) decreases significantly from 60 ± 2% to 12 ± 4% (i.e., 5 mmol kg^{-1}, Table 2). A subsequent decrease of the Fe(III) fraction with increasing metal loading was previously shown on IFM.[26,41] The fact that the amount of surface-bound Fe(III) of about 5 mmol kg^{-1} remains constant and independent of the Fe loadings, might indicate that oxidative processes are mainly taking place on the strong edge sites (≡S^{S}OH, ∼2−4 mmol kg^{-1}).[32] However, in case of Fe-low STx it cannot be excluded that the amount of surface-bound Fe(III) is limited by the availability of redox-active structural Fe(III). In addition to the presence of Fe(II) and Fe(III) doublets, a minor sextet appears in the Mössbauer spectrum at the higher loaded sample (Figure 3b). Sextets are rarely observed for low Fe-content clay minerals and are indicative of the presence of iron (hydr)-oxides.[19,39] The fitted hyperfine parameters of the sextet best match those of magnetite,[42] although it is difficult to conclusively assign the phase due to its relatively small spectral area.

Mössbauer Analysis of SWy. The fate of the sorbed Fe(II) on SWy was investigated by Mössbauer spectroscopy at 49 mmol kg^{-1} (^{57}Fe SWy a) and 130 mmol kg^{-1} (^{57}Fe SWy b).

dx.doi.org/10.1021/es501887q | Environ. Sci. Technol. 2014, 48, 8688−8697

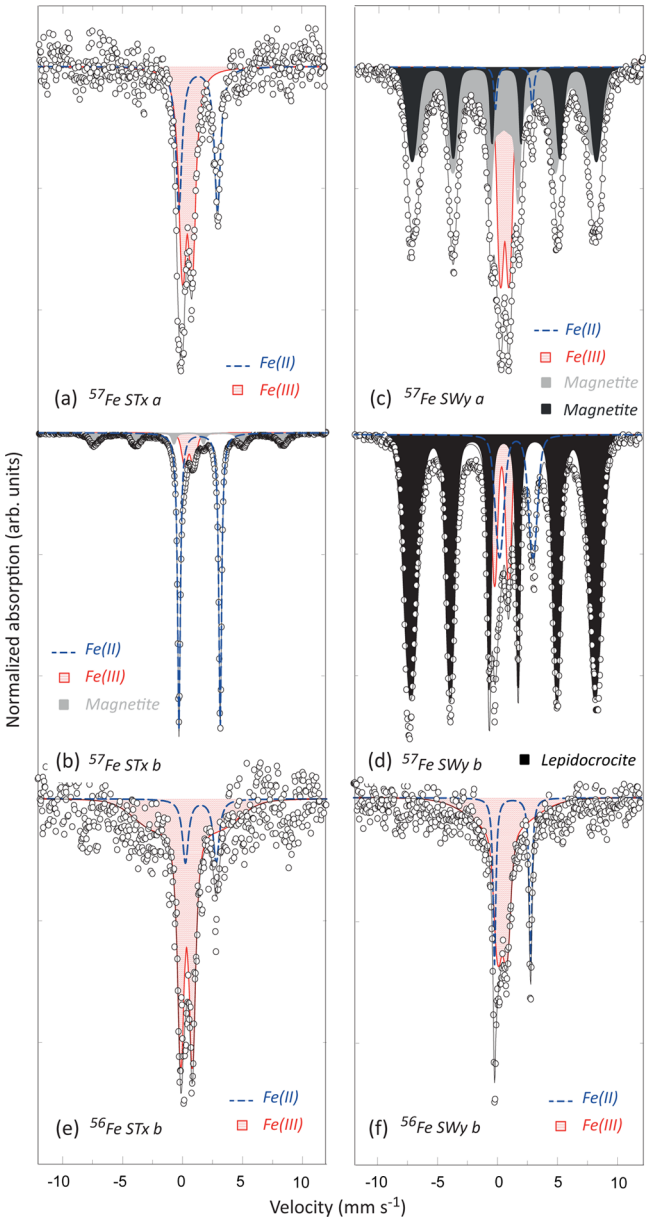

Figure 3. Mössbauer spectra of STx reacted with ^{57}Fe(II) at ^{57}Fe loadings of (a) 9.5 mmol kg^{-1} (^{57}Fe STx a) and (b) 39.8 mmol kg^{-1} (^{57}Fe STx b) to investigate Fe surface complexes. Mössbauer spectra of SWy reacted with ^{57}Fe(II) at ^{57}Fe loadings of (c) 49.0 mmol kg^{-1} (^{57}Fe SWy a) and (d) 128.8 mmol kg^{-1} (^{57}Fe SWy b). The corresponding Mössbauer spectra of STx and SWy reacted with invisible ^{56}Fe(II) in order to investigate the structural Fe are shown in parts e and f below (^{56}Fe STx b and ^{56}Fe SWy b).

At medium loadings (^{57}Fe SWy a), features reminiscent of clay-bound Fe(III) phases are overlaid by two six-line patterns (Figure 3c). Both sextets together comprise most of the spectral area (~80 ± 6%). The corresponding hyperfine parameters are close to literature values for magnetite (Fe_3O_4),[20] we cannot conclusively rule out the possibilities of other Fe(III) oxides, such as ferrihydrite or goethite.[43] In conclusion, the uptake of ^{57}Fe(II) resulted in a complete conversion of the sorbed Fe(II) to surface bound Fe(III) phases on SWy (~98.0%).

The higher loaded sample ^{57}Fe SWy b exhibits a similar Mössbauer signal (Figure 3d), except that the magnetic ordered phases could be modeled using only one sextet (CS 0.48 mm s^{-1} and QS −0.03 mm s^{-1}). According to the hyperfine parameters, the Fe(III) oxide phase is consistent with lepidocrocite (γ-FeOOH). The formation of clay bound lepidocrocite was previously shown by XRD and TEM in a study investigating the interaction of Fe(II) with NAu nontronite.[19] Regardless of whether the phase is a mixture of magnetite or lepidocrocite, it is obvious that ^{57}Fe(II) was oxidized to Fe(III) on the montmorillonite surface (~90.7%, Table 2). The amounts of surface bound Fe(III) species on SWy, which are not belonging to Fe(III) oxides, are similar and comparable with the values on STx (~9−14 mmol kg^{-1} vs 6 mmol kg^{-1}).

Interfacial Fe(II)−Fe(III) Electron Transfer. To investigate the extent of structural Fe(III) reduction, additional spectroscopic measurements were performed on STx and SWy samples equilibrated with Mössbauer invisible ^{56}Fe(II). The Fe(II) doublet in the ^{56}Fe STx b sample (Figure 3e) contributes to 27 ± 6% of the spectral area, suggesting that approximately 27% of the structural Fe in STx was reduced by the sorbed ^{56}Fe(II). The amount of structurally reduced Fe(II) is, within error, in agreement with the amount of oxidized Fe(III) measured on the clay surface of the corresponding ^{57}Fe STx b sample (Table 2). This result was confirmed by ^{56}Fe(II) sorption measurements on SWy (Figure 3f). In a similar way as for STx, the electrons released by the oxidation of the sorbed Fe(II) are equal to the electrons gained from the reduction of structural Fe(III). Approximately 117 mmol kg^{-1} (91 ± 5%) of the 129 mmol kg^{-1} sorbed Fe was oxidized (^{57}Fe SWy b, Table 2) which is, within error, consistent with the reduced 135 mmol kg^{-1} (26 ± 2%) of the total 521 mmol kg^{-1} structural Fe in the corresponding ^{56}Fe SWy b sample (Tables 1 and 2). This study shows that only up to 32 mmol kg^{-1} (i.e., 30%) of the structural Fe(III) is reduced to Fe(II) through oxidation of surface bound Fe(II) to Fe(III). This is in contrast with the work of Schaefer et al.[19] where a linear correlation was observed until ~516 mmol kg^{-1} (15%) of the structural Fe is reduced. A plausible explanation for this discrepancy can be derived from a recent study indicating that sorbed Fe(II) is not a strong enough reductant to reduce all the structural Fe(III).[10] Furthermore, electron transfer reactions may be inhibited by newly formed Fe precipitates on the clay surface.[8] It should be noted that Schaefer et al.[19] investigated the interfacial electron transfer on nontronite which is characterized by a much higher Fe content (~19.2 wt %) than SWy (~2.9 wt %) and the ^{56}Fe(II) loadings (~710 mmol kg^{-1}) were significantly higher than in this study (up to 195 mmol kg^{-1}).

EXAFS Analysis of STx and SWy Montmorillonites. *Structural Fe.* k^3-Weighted EXAFS spectra of structural Fe in STx and SWy montmorillonite exhibit a similar wave shape, except that the splitting of the oscillation at ~6 Å^{-1} is less pronounced for STx (Figure 4a).[44] In the corresponding radial structure functions (RSF), the backscattering peak at $R + \Delta R$ ~ 1.54 Å is attributed to the first Fe−O shell, while further peaks in the range between 2 and 5 Å are predominantly due to Fe−Al and Fe−Si single-scattering contributions (Figure 4a, below). In both samples, the local structural environment of the structural Fe is similar which is characteristic of octahedrally coordinated Fe (i.e., STx 5.8 ± 1.2 O at 2.00 ± 0.02 Å, 2.3 ± 1.6 Al at 2.99 ± 0.05 Å, 4.0 ± 1.7 Si at 3.20 ± 0.03 Å and SWy 4.9 ± 1.3 O at 1.99 ± 0.02 Å, 2.1 ± 2.2 Al at 3.03 ± 0.11 Å, 3.0 ± 2.1 Si at 3.20 ± 0.08 Å).[44] In contrast to the work of Vantelon et al.,[44] Fe−Fe backscattering pairs were not

dx.doi.org/10.1021/es501887q | Environ. Sci. Technol. 2014, 48, 8688−8697

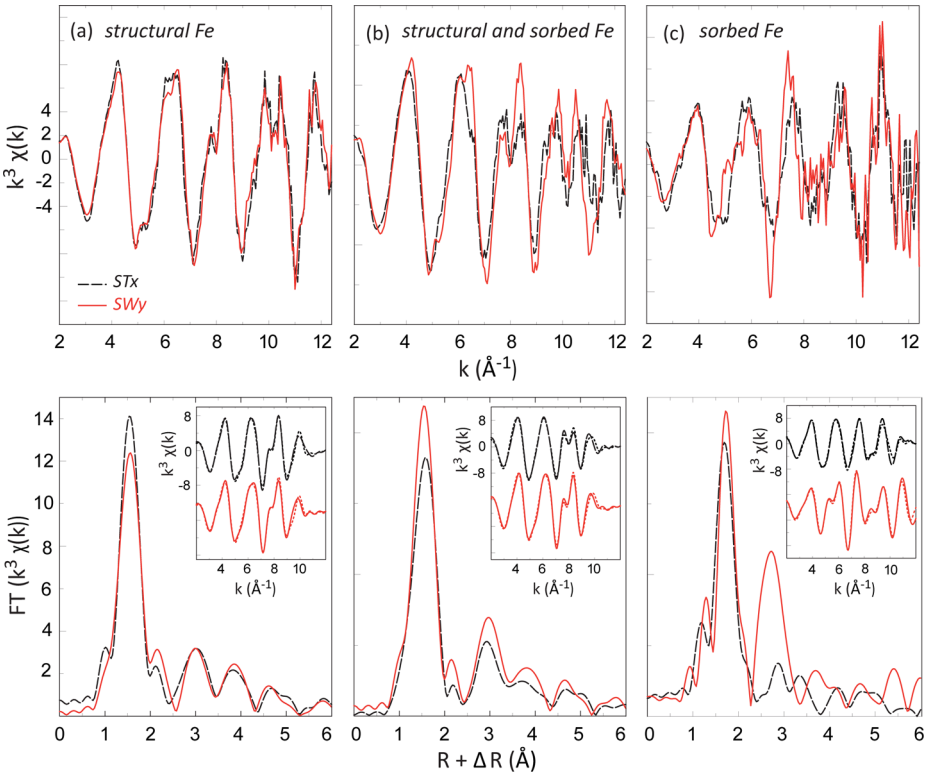

Figure 4. k^3-Weighted Fe K-edge EXAFS spectra obtained for (a) structural Fe (references), (b) structural and sorbed Fe (Fe STx c and Fe SWy c in Table 1), and (c) sorbed Fe. The EXAFS signals of STx are represented by dashed lines and the spectra of SWy by solid lines. The corresponding FT and FT^{-1} EXAFS data including the least-squares fit (dotted lines) are shown in the figures below and in the inset, respectively.

necessary to successfully fit the data of STx. Detailed structural informations about the EXAFS fit approach are given in Table S2 and S3 in the SI.

Surface Bound Fe. The EXAFS spectra illustrated in Figure 4b results from two Fe species, that is, structural and sorbed Fe. The structural Fe contributes to approximately 45.6% of the total EXAFS signal for the STx sample, respectively, 72.6% for the SWy sample (Table 1). In comparison to SWy, the splitting at 8 $Å^{-1}$ is more pronounced in the k^3-weighted spectra of the STx sample (Figure 4b). A similar trend was previously shown in a study investigating structural Fe in natural montmorillonites. In this study the observed shoulder was attributed to interferences resulting from two shells of the same cation located at different distances.[44] After the interaction with aqueous Fe(II), both k^3-weighted spectra show an enhanced splitting of the oscillation at ~10 $Å^{-1}$. Theoretical calculations indicated that this feature is correlated with an increased contribution of Fe as first octahedral neighbor.[44] However, taken into account the contribution of the structural Fe to the EXAFS signal, it is impossible to draw firm conclusions. For this reason, the overall signal of the total Fe (Figure 4b) was subtracted by the contribution of the structural Fe (Figure 4a) in order to analyze the signal of the Fe surface complexes separately as shown in Figure 4c (e.g., $\chi(k)_{surface} = (\chi(k)_{total} - 0.456\chi(k)_{structural})/0.544$, where $\chi(k)$ is the EXAFS signal of the STx samples, see also Table 1).[38] The Fe K-edge spectra of the structural Fe(III)-bearing montmorillonites were taken as references, although the presence of structural Fe(II) cannot be excluded in the Fe-loaded clay samples because of electron transfer reactions (up to 27% as demonstrated by Mössbauer spectroscopy, Table 2).

EXAFS analysis indicated that the Fe sorbed on STx is surrounded by 3.5 ± 0.2 O at 2.13 ± 0.01 Å, 0.8 ± 0.5 Al at 2.96 ± 0.04 Å, and 1.1 ± 0.5 Si at 3.23 ± 0.03 Å, which is characteristic for octahedrally located cations (Table S2, SI).[38,45,46] The slightly decreased coordination numbers in comparison to the structural Fe are characteristic for the formation of Fe complexes at the clay edge sites.[26] The interatomic distances agree well with the environment of the incorporated Fe except that in case of the surface bound Fe the distance to the first O shell is significantly increased from 2.00 ± 0.02 to 2.13 ± 0.01 Å. Typical Fe−O distances for the structural Fe in montmorillonite are, depending on the redox state, about 2.01 Å for Fe(III) and 2.10 Å for Fe(II).[26,47,48] The obtained Fe−O distance of ~2.13 strongly suggests that the iron surface complex on STx is predominantly present as Fe(II), confirming Mössbauer spectroscopy results.

By contrast, significant changes in the spectral shape and frequency of the k^3-weighted EXAFS spectra were observed for Fe taken up by SWy (Figure 4c, solid line). A new beat pattern at ~5 $Å^{-1}$ and multifrequency wave shape were formed in the EXAFS signal of the sorbed Fe. The appearance of a distinct feature has been observed in previous studies, which indicated the formation of precipitation products.[49−52] Clearly, the amplitude of the second peak in the RSF is significantly increased compared to the STx sample that is characteristic of a strong Fe−Fe contribution (Figure 4c, below). The radial structure function was successfully fitted using only Fe−O and Fe−Fe backscattering pairs (Table S3, SI). The surface bound Fe on SWy is surrounded by ~3.2 ± 0.3 O at 2.15 ± 0.01 Å, 6.6 ± 1.0 Fe at 3.12 ± 0.01 Å, and 2.5 ± 1.3 Fe at 3.57 ± 0.03 Å. The quality of the fit could be increased when the second peak in the RSF was fitted with an additional distant O shell at 3.32

dx.doi.org/10.1021/es501887q | Environ. Sci. Technol. 2014, 48, 8688−8697

± 0.02 Å. The coordination environment is comparable with the local structure of Fe oxide precipitates which is in agreement with the Mössbauer spectroscopy measurements.[53,54] Although the obtained Fe−O distance of ∼2.15 Å might indicate the formation of a ferrous (hydr)oxide, the reddish coloring observed in the high Fe loaded samples argues for the predominance of precipitated ferric oxides. Nevertheless, the calculated $\chi(k)$ spectra of the Fe surface complexes on SWy is too noisy to draw firm conclusions out of the fit results.

Structural Fe Properties and Implications on the Fe(II) Uptake. In the case of the low Fe-content montmorillonites, the Fe(II) uptake agrees well with the sorption behavior of other divalent transition metals,[18,26] even though sorbed Fe(II) is partially oxidized to mineral-bound Fe(III) complexes (up to 6 mmol kg^{-1}). For the Fe-rich montmorillonites, the sorption of Fe(II) is more pronounced and Fe(II) taken up by the clay surface was fully oxidized (up to 117 mmol kg^{-1}). In both Fe-low and Fe-rich clays, the oxidation of the sorbed Fe(II) is mainly caused by an electron transfer to the structural Fe(III). An enhanced structural Fe redox activity, which results in complete oxidation of the sorbed Fe(II), is therefore the most probable reason for the unexpected high sorption values on certain Fe-bearing clay minerals. Two plausible reasons are proposed to explain discrepancies in the redox properties of the STx and SWy montmorillonites used. Either the redox capacity of the clay mineral depends on multiple structural parameters including the Fe(III) content (0.5 vs 2.9 wt %)[10] or the structural Fe in STx is less accessible for an interfacial electron transfer than in SWy due to differences in the clay structure (e.g., Fe clustering or random distribution of Fe). This last hypothesis is supported by the findings of Vantelon et al.[44] in which SWy displays an ordered distribution of Fe atoms in the clay lattice, while the structural Fe in STx is characterized by a close to random distribution. Several studies have recently emphasized that there is a correlation between the redox activity of structural Fe and the applied redox conditions (E_h).[4,10] The observations in this study raise the question of how is the sorption behavior on montmorillonites controlled by the reduction potential (E_h) in biogeochemical systems.

Finally, the results indicate that an increased Fe(II) sorption may be expected for most Fe(III)-rich clay minerals, which significantly underscores their importance as Fe(II) sinks and the role of mineral-bound Fe(III) as potential oxidant for inorganic and organic contaminants in anoxic geochemical environments. For example, the presence of high amounts of sorbed Fe may significantly influence the retardation of metal and radioactive contaminants through competitive sorption effects (e.g., radioactive waste repositories). The findings suggest that the extent of Fe(II) uptake is more clay-specific and more complex than previously considered. The complexity of Fe(II) reactions at the montmorillonite-water interface requires us to reassess previous sorption models of divalent metals and their applicability for describing the Fe(II) uptake on natural clays. The sorption of ferrous iron on clay minerals cannot be accurately modeled without considering both the fate of the Fe surface species and the structural Fe redox properties and coordination environments. Clearly, a more dynamic clay-type specific description including Fe(II)/clay redox cycling is required for future modeling approaches.

■ ASSOCIATED CONTENT

Supporting Information

Details on the K-edge EXAFS analysis, additional Mössbauer and EXAFS spectra, and wet chemistry experiments at different pH on natural and dithionite-treated clay minerals. This material is available free of charge via the Internet at http://pubs.acs.org.

■ AUTHOR INFORMATION

Corresponding Author

*E-mail: daniela.soltermann@psi.ch. Phone: +41-56-310-2285, Fax: +41-56-310-3565.

Notes

The authors declare no competing financial interest.

■ ACKNOWLEDGMENTS

Elmotaz Etlayeb is thanked for his contribution to the experimental work. Financial support was provided by the Swiss National Science Foundation.

■ REFERENCES

(1) Hofstetter, T. B.; Neumann, A.; Schwarzenbach, R. P. Reduction of nitroaromatic compounds by Fe(II) species associated with iron-rich smectites. *Environ. Sci. Technol.* **2006**, *40* (1), 235−242.

(2) Neumann, A.; Olson, T. L.; Scherer, M. M. Spectroscopic evidence for Fe(II)-Fe(III) electron transfer at clay mineral edge and basal sites. *Environ. Sci. Technol.* **2013**, *47* (13), 6969−6977.

(3) Gorski, C. A.; Kluepfel, L.; Voegelin, A.; Sander, M.; Hofstetter, T. B. Redox properties of structural Fe in clay minerals. 2. Electrochemical and spectroscopic characterization of electron transfer irreversibility in ferruginous smectite, SWa-1. *Environ. Sci. Technol.* **2012**, *46* (17), 9369−9377.

(4) Gorski, C. A.; Aeschbacher, M.; Soltermann, D.; Voegelin, A.; Baeyens, B.; Marques Fernandes, M.; Hofstetter, T. B.; Sander, M. Redox properties of structural Fe in clay minerals. 1. Electrochemical quantification of electron-donating and -accepting capacities of smectites. *Environ. Sci. Technol.* **2012**, *46* (17), 9360−9368.

(5) Hofstetter, T. B.; Schwarzenbach, R. P.; Haderlein, S. B. Reactivity of Fe(II) species associated with clay minerals. *Environ. Sci. Technol.* **2003**, *37* (3), 517−528.

(6) Bishop, M. E.; Dong, H.; Kukkadapu, R. K.; Liu, C.; Edelmann, R. E. Bioreduction of Fe-bearing clay minerals and their reactivity toward pertechnetate (Tc-99). *Geochim. Cosmochim. Acta* **2011**, *75* (18), 5229−5246.

(7) Pentrakova, L.; Su, K.; Pentrak, M.; Stuck, J. W. A review of microbial redox interactions with structural Fe in clay minerals. *Clay Miner.* **2013**, *48* (3), 543−560.

(8) Dong, H.; Jaisi, D. P.; Kim, J.; Zhang, G. Microbe-clay mineral interactions. *Am. Mineral.* **2009**, *94* (11−12), 1505−1519.

(9) Neumann, A.; Hofstetter, T. B.; Luessi, M.; Cirpka, O. A.; Petit, S.; Schwarzenbach, R. P. Assessing the redox reactivity of structural iron in smectites using nitroaromatic compounds as kinetic probes. *Environ. Sci. Technol.* **2008**, *42* (22), 8381−8387.

(10) Gorski, C. A.; Kluepfel, L. E.; Voegelin, A.; Sander, M.; Hofstetter, T. B. Redox properties of structural Fe in clay minerals: 3. Relationships between smectite redox and structural properties. *Environ. Sci. Technol.* **2013**, *47* (23), 13477−13485.

(11) Pecher, K.; Haderlein, S. B.; Schwarzenbach, R. P. Reduction of polyhalogenated methanes by surface-bound Fe(II) in aqueous suspensions of iron oxides. *Environ. Sci. Technol.* **2002**, *36* (8), 1734−1741.

(12) Bürge, I. J.; Hug, S. J. Influence of mineral surfaces on Chromium(VI) reduction by Iron(II). *Environ. Sci. Technol.* **1999**, *33* (23), 4285−4291.

(13) Hofstetter, T. B.; Heijman, C. G.; Haderlein, S. B.; Holliger, C.; Schwarzenbach, R. P. Complete reduction of TNT and other

(poly)nitroaromatic compounds under iron reducing subsurface conditions. *Environ. Sci. Technol.* **1999**, *33* (9), 1479−1487.
(14) Amonette, J. E.; Workman, D. J.; Kennedy, D. W.; Fruchter, J. S.; Gorby, Y. A. Dechlorination of carbon tetrachloride by Fe(II) associated with goethite. *Environ. Sci. Technol.* **2000**, *34* (21), 4606−4613.
(15) Schultz, C.; Grundl, T. pH dependence of ferrous sorption onto two smectite clays. *Chemosphere* **2004**, *57* (10), 1301−1306.
(16) Jaisi, D. P.; Dong, H. L.; Liu, C. X. Influence of biogenic Fe(II) on the extent of microbial reduction of Fe(III) in clay minerals nontronite, illite, and chlorite. *Geochim. Cosmochim. Acta* **2007**, *71* (5), 1145−1158.
(17) Jaisi, D. P.; Liu, C.; Dong, H.; Blake, R. E.; Fein, J. B. Fe^{2+} sorption onto nontronite (NAu-2). *Geochim. Cosmochim. Acta* **2008**, *72* (22), 5361−5371.
(18) Bradbury, M. H.; Baeyens, B. Modelling the sorption of Mn(II), Co(II), Ni(II), Zn(II), Cd(II), Eu(III), Am(III), Sn(IV), Th(IV), Np(V) and U(VI) on montmorillonite: Linear free energy relationships and estimates of surface binding constants for some selected heavy metals and actinides. *Geochim. Cosmochim. Acta* **2005**, *69* (4), 875−892.
(19) Schaefer, M. V.; Gorski, C. A.; Scherer, M. M. Spectroscopic evidence for interfacial Fe(II)-Fe(III) electron transfer in a clay mineral. *Environ. Sci. Technol.* **2011**, *45* (2), 540−545.
(20) Gorski, C. A.; Scherer, M. M. Influence of magnetite stoichiometry on Fe-II uptake and nitrobenzene reduction. *Environ. Sci. Technol.* **2009**, *43* (10), 3675−3680.
(21) Handler, R. M.; Beard, B. L.; Johnson, C. M.; Scherer, M. M. Atom exchange between aqueous Fe(II) and goethite: An Fe isotope tracer study. *Environ. Sci. Technol.* **2009**, *43* (4), 1102−1107.
(22) Larese-Casanova, P.; Scherer, M. M. Fe(II) sorption on hematite: New insights based on spectroscopic measurements. *Environ. Sci. Technol.* **2007**, *41* (2), 471−477.
(23) Soltermann, D.; Baeyens, B.; Bradbury, M. H.; Marques Fernandes, M. Fe(II) uptake on natural montmorillonites. II. Surface complexation modeling. *Environ. Sci. Technol.* **2014**, DOI: 10.1021/es501902f.
(24) Reinholdt, M.; Miehe-Brendle, J.; Delmotte, L.; Tuilier, M. H.; le Dred, R.; Cortes, R.; Flank, A. M. Fluorine route synthesis of montmorillonites containing Mg or Zn and characterization by XRD, thermal analysis, MAS NMR, and EXAFS spectroscopy. *Eur. J. Inorg. Chem.* **2001**, *11*, 2831−2841.
(25) Reinholdt, M.; Miehe-Brendle, J.; Delmotte, L.; Le Dred, R.; Tuilier, M. H. Synthesis and characterization of montmorillonite-type phyllosilicates in a fluoride medium. *Clay Miner.* **2005**, *40* (2), 177−190.
(26) Soltermann, D.; Marques Fernandes, M.; Baeyens, B.; Dähn, R.; Miehé-Brendlé, J.; Wehrli, B.; Bradbury, M. H. Fe(II) sorption on a synthetic montmorillonite. A combined macroscopic and spectroscopic study. *Environ. Sci. Technol.* **2013**, *47* (13), 6978−6986.
(27) Bradbury, M. H.; Baeyens, B. A mechanistic description of Ni and Zn sorption on Na-montmorillonite 0.2. Modelling. *J. Contam. Hydrol.* **1997**, *27* (3−4), 223−248.
(28) Bradbury, M. H.; Baeyens, B. Experimental measurements and modeling of sorption competition on montmorillonite. *Geochim. Cosmochim. Acta* **2005**, *69* (17), 4187−4197.
(29) Baeyens, B.; Bradbury, M. H. Cation exchange capacity measurements on Illite using the sodium and cesium isotope dilution technique: Effects of the index cation, electrolyte concentration and competition: Modeling. *Clays Clay Miner.* **2004**, *52* (4), 421−431.
(30) Stucki, J. W.; Golden, D. C.; Roth, C. B. Preparation and handling of dithionite-reduced smectite suspensions. *Clays Clay Miner.* **1984**, *32* (3), 191−197.
(31) Perrin, D. D.; Dempsey, B. *Buffers for pH and Metal Ion Control*; Chapman & Hall: London, 1974.
(32) Baeyens, B.; Bradbury, M. H. A mechanistic description of Ni and Zn sorption on Na-montmorillonite 0.1. Titration and sorption measurements. *J. Contam. Hydrol.* **1997**, *27* (3−4), 199−222.
(33) Bradbury, M. H.; Baeyens, B. Discussion on: ″A mechanistic description of Ni and Zn sorption on Na-montmorillonite. Part I: Titration and sorption measurements. Part II: Modelling″ by Bart Baeyens and Michael H. Bradbury - Reply to some comments. *J. Contam. Hydrol.* **1997**, *28* (1−2), 11−16.
(34) Rancourt, D. G.; Ping, J. Y. Voigt-based methods for arbitrary-shape static hyperfine parameter distributions in Mössbauer spectroscopy. *Nucl. Instrum. Methods Phys. Res. Sect. B* **1991**, *58* (1), 85−97.
(35) Newville, M. IFEFFIT: Interactive XAFS analysis and FEFF fitting. *J. Synchrotron Radiat.* **2001**, *8*, 322−324.
(36) Ravel, B.; Newville, M. ATHENA, ARTEMIS, HEPHAESTUS: Data analysis for X-ray absorption spectroscopy using IFEFFIT. *J. Synchrotron Radiat.* **2005**, *12*, 537−541.
(37) Bradbury, M. H.; Baeyens, B. Modelling the sorption of Zn and Ni on Ca-montmorillonite. *Geochim. Cosmochim. Acta* **1999**, *63* (3−4), 325−336.
(38) Dähn, R.; Baeyens, B.; Bradbury, M. H. Investigation of the different binding edge sites for Zn on montmorillonite using P-EXAFS - The strong/weak site concept in the 2SPNE SC/CE sorption model. *Geochim. Cosmochim. Acta* **2011**, *75* (18), 5154−5168.
(39) Murad, E.; Cashion, J. *Mössbauer Spectroscopy of Environmental Materials and their Industrial Utilization*; Kluwer: Dordrecht, 2006.
(40) Charlet, L.; Tournassat, C. Fe(II)-Na(I)-Ca(II) cation exchange on montmorillonite in chloride medium: Evidence for preferential clay adsorption of chloride - metal ion pairs in seawater. *Aquatic Geochem.* **2005**, *11* (2), 115−137.
(41) Géhin, A.; Greneche, J. M.; Tournassat, C.; Brendle, J.; Rancourt, D. G.; Charlet, L. Reversible surface-sorption-induced electron-transfer oxidation of Fe(II) at reactive sites on a synthetic clay mineral. *Geochim. Cosmochim. Acta* **2007**, *71* (4), 863−876.
(42) Cornell, R. M.; Schwertmann, U. *The Iron Oxides: Structure, Properties, Reactions, Occurences and Uses*, 2nd, ed.; Wiley-VCH: Weinheim, 2003.
(43) Murad, E.; Schwertmann, U. The influence of crystallinity on the Mössbauer spectrum of lepidocrocite. *Mineral. Mag.* **1984**, *48* (349), 507−511.
(44) Vantelon, D.; Montarges-Pelletier, E.; Michot, L. J.; Briois, V.; Pelletier, M.; Thomas, F. Iron distribution in the octahedral sheet of dioctahedral smectites. An Fe K-edge X-ray absorption spectroscopy study. *Phys. Chem. Miner.* **2003**, *30* (1), 44−53.
(45) Schlegel, M. L.; Manceau, A.; Charlet, L.; Hazemann, J. L. Adsorption mechanisms of Zn on hectorite as a function of time, pH, and ionic strength. *Am. J. Sci.* **2001**, *301* (9), 798−830.
(46) Schlegel, M. L.; Manceau, A. Evidence for the nucleation and epitaxial growth of Zn phyllosilicate on montmorillonite. *Geochim. Cosmochim. Acta* **2006**, *70* (4), 901−917.
(47) Manceau, A.; Lanson, B.; Drits, V. A.; Chateigner, D.; Gates, W. P.; Wu, J.; Huo, D.; Stucki, J. W. Oxidation-reduction mechanism of iron in dioctahedral smectites: I. Crystal chemistry of oxidized reference nontronites. *Am. Mineral.* **2000**, *85* (1), 133−152.
(48) Manceau, A.; Drits, V. A.; Lanson, B.; Chateigner, D.; Wu, J.; Huo, D.; Gates, W. P.; Stucki, J. W. Oxidation-reduction mechanism of iron in dioctahedral smectites: II. Crystal chemistry of reduced Garfield nontronite. *Am. Mineral.* **2000**, *85* (1), 153−172.
(49) Dähn, R.; Scheidegger, A.; Manceau, A.; Schlegel, M. L.; Baeyens, B.; Bradbury, M. H.; Morales, M. Neoformation of Ni phyllosilicate upon Ni uptake on montmorillonite: A kinetics study by powder and polarized extended X-ray absorption fine structure spectroscopy. *Geochim. Cosmochim. Acta* **2003**, *67* (10), 1935−1935.
(50) Schlegel, M. L.; Manceau, A.; Charlet, L.; Chateigner, D.; Hazemann, J. L. Sorption of metal ions on clay minerals. III. Nucleation and epitaxial growth of Zn phyllosilicate on the edges of hectorite. *Geochim. Cosmochim. Acta* **2001**, *65* (22), 4155−4170.
(51) Scheinost, A. C.; Ford, R. G.; Sparks, D. L. The role of Al in the formation of secondary Ni precipitates on pyrophyllite, gibbsite, talc, and amorphous silica: A DRS study. *Geochim. Cosmochim. Acta* **1999**, *63* (19−20), 3193−3203.
(52) Scheidegger, A. M.; Strawn, D. G.; Lamble, G. M.; Sparks, D. L. The kinetics of mixed Ni-Al hydroxide formation on clay and

aluminum oxide minerals: A time-resolved XAFS study. *Geochim. Cosmochim. Acta* **1998**, *62* (13), 2233−2245.
(53) Manceau, A.; Nagy, K. L.; Spadini, L.; Ragnarsdottir, K. V. Influence of anionic layer structure of Fe-oxyhydroxides on the structure of Cd surface complexes. *J. Colloid Interface Sci.* **2000**, *228* (2), 306−316.
(54) Peacock, C. L.; Sherman, D. M. Copper(II) sorption onto goethite, hematite and lepidocrocite: A surface complexation model based on ab initio molecular geometries and EXAFS spectroscopy. *Geochim. Cosmochim. Acta* **2004**, *68* (12), 2623−2637.